

Experimental Investigation of HFRP Composite Beams

Hiroshi Mutsuyoshi, Nguyen Duc Hai, Kensuke Shiroki, Thiru Aravinthan, and
Allan Manalo

Synopsis: This paper presents the development of composite beams using hybrid CFRP/GFRP (HFRP) I-beam and Normal Strength Concrete (NSC) slab and precast Ultra-High Performance fiber reinforced Concrete (UHPFRC) slab. UHPFRC has high strength and high ductility allowing for a reduction in the cross-sectional area and self weight of the beam. A number of full-scale flexural beam tests were conducted using different dimensions of slab and with/without epoxy bonding between the slab and HFRP I-beam. The test results suggested that the flexural stiffness of composite beams with bolted and bonded shear connection is higher than that with bolted-only shear connection. Delamination failure was not observed in the compressive flange of the HFRP I-beam and the high tensile strength of CFRP in the bottom flange was effectively utilized with the addition of the UHPFRC slab on the top flange.

Keywords: Composite beam, hybrid fiber reinforced polymer, normal strength concrete, ultra-high performance fiber-reinforced concrete, flexural stiffness

Biographical information

Dr. Hiroshi Mutsuyoshi is a Professor at the Department of Civil and Environmental Engineering at Saitama University, Japan. He received his doctoral degree in Engineering from the University of Tokyo in 1984. He is the president of the Japan Reinforcing Bar Joints Institute. He is a member of the ACI International Partnership Committee, 440 Committee and a convener of TG 9.14 (extradosed tendons) of fib-Commission 9 (Reinforcing and Prestressing Materials and Systems).

Dr. Nguyen Duc Hai is a postdoctoral research fellow at Saitama University. He obtained his PhD degree from Saitama University in 2010. His research interests include FRP composites in structural engineering, testing and FE analysis of FRP composite structures, mechanics of composite materials and structures, innovative bridge materials and strengthening and rehabilitation of civil infrastructures using FRP composites. He is a member of the International Institute for FRP in Construction (IIFC).

Mr. Kensuke Shiroki is a structural engineer at Japan Railway Construction, Transport and Technology Agency. He achieved his master's degree in civil engineering at Saitama University in 2010. He is a member of the Japan Concrete Institute (JCI).

Dr. Thiru Aravinthan is an Associate Professor in Engineered Fibre Composites affiliated with CEEFC, at the University of Southern Queensland in Toowoomba, Australia. He leads major R&D projects in the CEEFC especially on the application of fibre composite materials in civil infrastructure and leading the education and training within CEEFC. He has more than 20 years of combined research, industry and teaching experience in structural and materials engineering. He is a Chartered Professional Engineer in Civil and Structural Engineering and a registered Professional Engineer at Oregon State, USA.

Mr. Allan Manalo is a PhD student at the CEEFC at the University of Southern Queensland (USQ), Toowoomba, Australia. He was awarded a Master's in Engineering

Degree in March 2008 after completing a research work on hybrid FRP composites bridge girder at Saitama University, Japan. He joined USQ in April 2008 to pursue a doctoral degree in structural engineering and currently doing research on the behavior of fibre composite sandwich beams for structural applications.

INTRODUCTION

Fiber Reinforced Polymer (FRP) has several advantages such as high strength, light weight and corrosion resistance. In recent years, FRP materials have been applied to structural members in many pedestrian and road bridges. Presently, a hybrid FRP (HFRP) composite beam for bridge girder applications is being developed. This beam optimizes the combined use of Carbon Fiber Reinforced Polymer (CFRP) and Glass Fiber Reinforced Polymer (GFRP) in a single wide-flange beam section. While CFRP has high tensile strength and stiffness, it is relatively expensive, whereas GFRP is comparatively less expensive but its mechanical properties are lower than those of CFRP. In a beam subjected to bending moment about the strong axis, the top and bottom flanges are subjected to high axial stress while the web is subjected to shear stress. In the HFRP beam, the flanges are fabricated using a combination of CFRP and GFRP layers. On the other hand, the web is composed entirely of GFRP because it is not subjected to the same high stresses. The HFRP beam therefore utilizes the advantages of both CFRP and GFRP for strength, stiffness and economy. The HFRP beam is expected to find its application in severe corrosive environments or where lightweight rapid construction is required. The application of HFRP composites could also contribute to a reduction of life cycle costs (LCC) of the structure and environmental load due to its low carbon dioxide emission (Sakai 2005; Tanaka et al. 2006).

This paper presents the flexural behavior of HFRP beams and composite behavior of HFRP beam and a topping slab. Two types of materials used for topping slab are considered including Normal Strength Concrete (NSC) and Ultra-High Performance fiber reinforced concrete (UHPC). Different dimensions of slab and with/without epoxy bonding between the slab and HFRP I-beam are utilized. A number of full-scale flexural

tests are performed and the test results are discussed focusing on flexural stiffness of the composite beams.

RESEARCH SIGNIFICANCE

Many infrastructures all over the world suffer from deterioration problems resulting in reduction of their service life. This problem has been severely affecting many bridges especially in the coastal areas. It is therefore urgent to apply sustainable materials to bridge structures to improve their durability. Accordingly, hybrid Fiber Reinforced Polymers (HFRP) beams consisted of CFRP and GFRP have been utilized in this study. The current work has provided valuable experimental data on flexural behavior of HFRP beams and composite action between HFRP beams and topping slabs. Ultra-High Performance fiber reinforced concrete (UHPFRC) was selected for the topping slab since it has a great potential in reducing self weight and improving flexural stiffness of HFRP-concrete structures.

FLEXURAL TEST OF HFRP BEAMS

HFRP Beams

The HFRP I-beams were manufactured by pultrusion process using the FRP layer composition shown in Table 1. The top and bottom flanges of the I-beam are composed of CFRP and GFRP in order to increase flexural strength and beam stiffness. All CFRP fibers in the flanges are aligned in the longitudinal direction (oriented at 0 degree) while the GFRP is oriented at 0, 90 and ± 45 degrees to provide integrity across the flange width, and avoid strong anisotropic behavior. The web is composed entirely of GFRP because of the lower stresses, and to reduce cost. The overall height of the HFRP beam is 250 mm and the flange width is 95 mm. The flange thickness is 14 mm and the web thickness is 9 mm (Figure 1). The mechanical properties of CFRP and GFRP are shown in Table 1. The effective mechanical properties of the HFRP laminates obtained from the material tests are shown in Table 2.

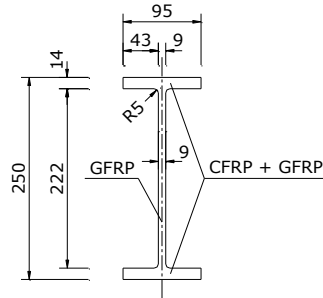


Figure 1—Dimensions of HFRP I-beams (mm)

Table 1—Mechanical properties of materials

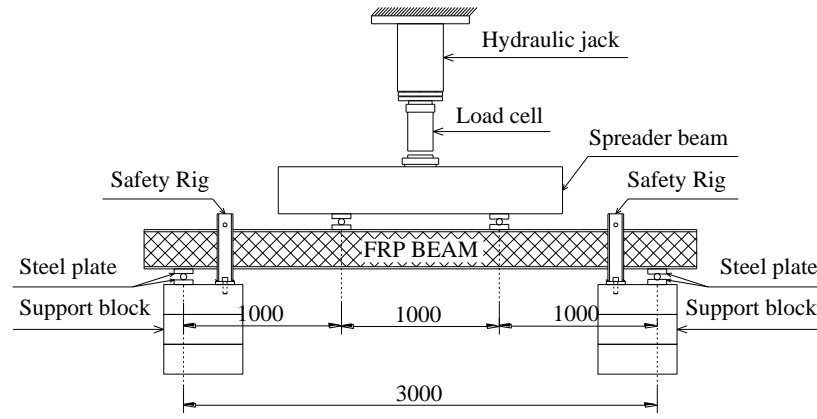
Parameters	Notation	CFRP	GFRP	GFRP	GFRP
		0°	0/90°	±45°	CSM
Volume Fraction	V_f (%)	55	53	53	25
Volume Content	Flange (%)	33	17	41	9
	Web (%)	0	43	43	14
Young's Modulus	E_{11} (GPa)	128.1	25.9	11.1	11.1
	E_{22} (GPa)	14.9	25.9	11.1	11.1
Shear Modulus	G_{12} (GPa)	5.5	4.4	10.9	4.2
Poisson's Ratio	ν_{12} (-)	0.32	0.12	0.58	0.31

Table 2—Effective Mechanical Properties of HFRP Laminates

	Flange	Web
Compressive strength (MPa)	394	299
Tensile strength (MPa)	884	185
Young's modulus (GPa)	49.6	17.8

Test Program

The beams were simply supported and tested in four-point bending at a span of 3,000 mm with an interior loading span of 1,000 mm. Web stiffeners were installed to prevent crippling and warping at the supports and local failure at the loading points. The timber stiffeners were bonded with FRP beam by epoxy adhesion. Safety rigs were installed near the supports to prevent beams from sudden falling in the case of any lateral buckling. The test setup is shown schematically in Figure 2. All beams were fabricated of CFRP and GFRP in the flanges and only GFRP in the web.



(a) Configuration



(b) Actual view

Figure 2—Test setup

Test Results and Discussions

Figure 3 shows the relationship between the load and mid-span deflection of the pultruded I-beam. It can be seen that the behavior of beam is almost linear up to the failure. The typical failure mode of pultruded beams is shown in Figures 4-5. It was crushing of fibers near the loading point due to load concentration followed by delamination of the compressive flange between the upper and lower part of the top flange. It seems that the load carrying capacity of the pultruded I-beam is not governed by the compressive or tensile strength of the FRP material but related with the bonding

strength at the interface between fiber layers. Finite Element Analysis (FEA) using MSC.Marc code has been conducted and showed good agreement with the experimental result. Indeed, the failure load of the HFRP beam obtained from FEA is approximately 200 kN which is only 2.5% difference compared with that of the experimental result.

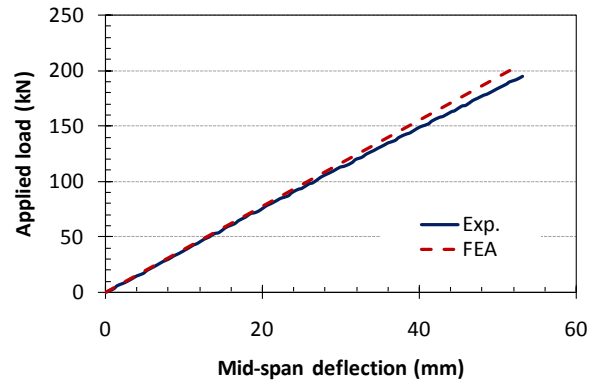


Figure 3—Load-deflection curve at mid-span section



Figure 4—Crushing of fibers and delamination

Figure 6 shows the relationship between load and longitudinal strain at the top and bottom flange at the mid-span section. The results indicate that both compressive and tensile strain behave linearly up to the failure. Both maximum compressive and tensile strains reach a value of approximately 6,100 microstrains, which is only 44% ultimate tensile strain of CFRP. Load versus longitudinal strain curves obtained from FEA show slightly stiffer behaviors than those obtained from the experiments. These differences could be due to imperfections of FRP layers in the manufacturing process of HFRP specimens.



Figure 5—Closer view of delamination

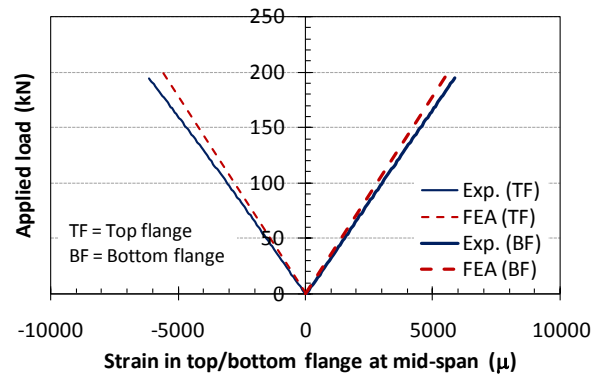


Figure 6—Load-longitudinal strain curve

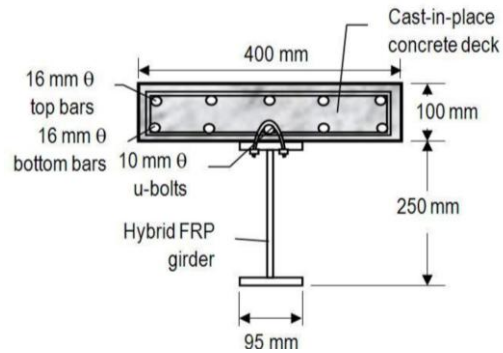
FLEXURAL TEST OF HFRP-NSC COMPOSITE BEAMS

As discussed in the previous section on the flexural behavior of HFRP beams, it was reported that the HFRP I-beams subjected to bending failed in the compressive flange due to delamination between the CFRP and the GFRP interface. These test results suggest that the individual HFRP beams could not utilize the high tensile strength of the CFRP in the tension flange. To fully utilize this strength, the delamination failure in the compression flange must be avoided. One approach to accomplish this is to reduce the stress in the HFRP compression flange by adding a concrete topping slab to resist the compressive forces. This is analogous to composite steel construction where compression buckling failure of the steel top flange can be avoided by using the concrete topping slab to carry compression force.

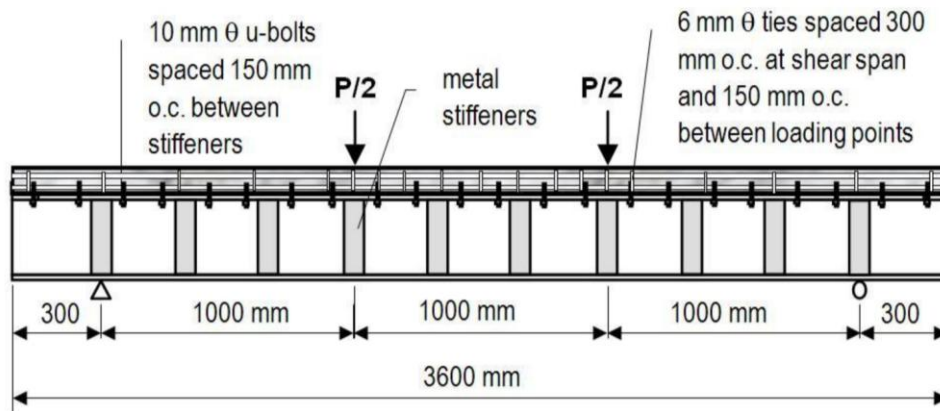
This section aims to develop a composite beam using HFRP I-beams and a Normal Strength Concrete (NSC) topping slab. It is expected that the composite beam system will increase beam stiffness, prevent buckling and delamination in the HFRP compressive flange and more effectively utilize the high tensile strength of the CFRP in the HFRP tension flange. Since the slab will carry most of compressive forces, it is no longer necessary to include CFRP in the top flange. However, during manufacturing of the HFRP I-beam, it was determined that the top and bottom flanges must have the same properties to avoid initial beam deformation after pultrusion process.

Test Specimen

Specimen HFRP-NSC represents the HFRP composite beam with cast-in-place NSC slab bonded with epoxy and steel u-bolts. The length of the HFRP beam is 3600 mm with a clear span of 3000 mm. High strength steel u-bolts made of 10 mm diameter and epoxy resin were used as shear connectors. The steel u-bolts were spaced at 150 mm. The top flange of the HFRP beam was sandpapered and cleaned with acetone to give a rough bond surface before the application of epoxy adhesives. The NSC slab was 100 mm thick and 400 mm wide with 10 steel bars (16 mm diameter bars) to provide additional compressive force on the concrete section. The NSC has a mean cylinder strength of 32 MPa obtained from compression test at 14 days (at the same age of testing the specimen). Five steel bars with 16 mm diameter were used in the bottom to delay the formation of tension cracks and limit the crack width on the NSC slab. Lateral steel ties with aspect of 300 mm in the shear span and 150 mm between the loading points were installed to provide confinement of concrete. The steel bars have an elastic modulus of 200 GPa and a yield strength of 300 MPa. The dimensions and configurations of the test specimen are shown in Figure 7.



(a) Cross section



(b) Loading configuration

Figure 7—Dimensions and configurations of specimen HFRP-NSC

Test Program

Four point bending test was conducted. The test setup is shown in Figure 8. A hydraulic jack was used to apply the load monotonically through a spreader beam. The deflection, strains and failure mode were recorded during loading and until failure of the specimen.

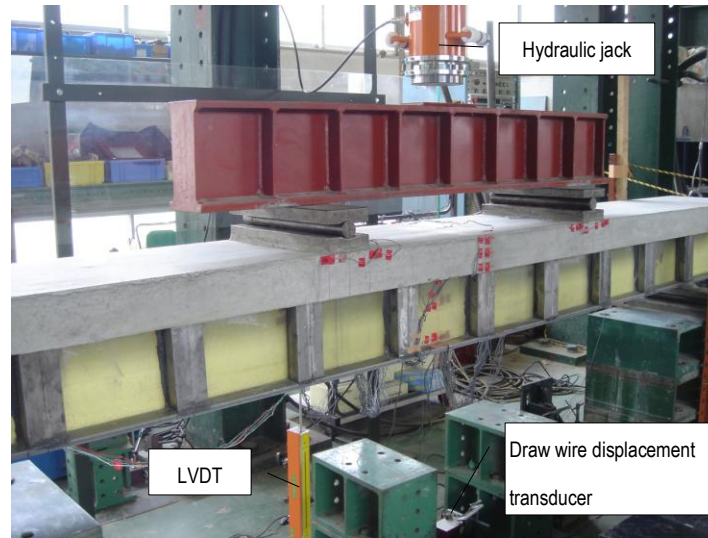


Figure 8—Test setup of HFRP-NSC

Test Results

The load and middle span deflection curve of HFRP beam with an overlying NSC slab is shown in Figure 9. Based on the figure, the load increased linearly with deflection until an applied load of 196 KN and a reduction in stiffness was observed until final failure. The reduced stiffness may be caused by the development of diagonal cracks within the shear span which contributed to the downward deflection of the beam. HFRP-NSC failed due to crushing of the concrete at the shear span followed by shear failure of the top flange and web of the HFRP beam at an applied load of 427 KN with a middle span deflection of 73.9 mm. Consequently, result of the experimental investigation showed that the composite action with a NSC slab could overcome deflection limitations inherent in HFRP beam and a higher load carrying capacity at final failure could be attained compared to HFRP beam alone.

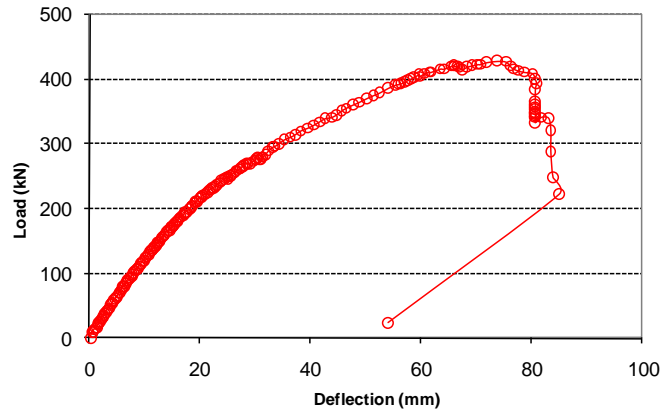


Figure 9—Load and middle span deflection curve of HFRP-NSC

Figure 10 shows the failure mode of HFRP composite beam with NSC slab. Development of diagonal cracks within the shear span started at a load of 196 KN. The crack width increased with the increase of load and lead to the compression failure of concrete slab near the loading point followed by shear failure on the top flange. Shear failure in the top flange of HFRP beam may be due to stress concentration in the holes provided for the u-bolts. This was not the expected failure mode as the HFRP composite beam was designed to fail by rupture of the HFRP in tension. However in actual design, this may be a preferable failure mode because cracks in the concrete slab will give an adequate warning of impending failure to the structure.



(a) Compression failure of NSC slab



(b) Shear failure of HFRP beam

Figure 10—Failure mode of specimen HFRP-NSC

FLEXURAL TEST OF HFRP-UHPFRC COMPOSITE BEAMS

The behaviors of composite beams using HFRP beam and NSC topping slab verified the importance of composite action in increasing the beam stiffness and utilizing the high tensile strength of the HFRP beam. These have been reported by Deskovic et al. (1995), Keller et al. (2007), Correia et al. (2007) as well. However, the use of NSC required a larger cross-sectional area for the deck to attain a tensile failure for HFRP, thus, resulted to a heavy composite beam system. In order to maintain the light weight of the HFRP beam in the composite beam, high performance concrete topping slab should be used. Elmahdy et al. (2008) investigated the behavior of the hybrid section consisted of GFRP pultruded hollow box section with Ultra High-Performance Concrete (UHPC) cast on top. Steel reinforced polymer sheet or CFRP sheet was applied at the base of the section. The results indicated that the application of UHPC and tensile reinforcement sheets increased the flexural capacity of the hybrid section by approximately 3.7 times when compared to the strength of the GFRP hollow section alone. Unfortunately, there have been very few works done so far on the behavior of hybrid FRP-UHPC system. This study aims to further investigate the composite behavior of this system for bridge applications. Ultra-High Performance Fiber Reinforced Concrete (UHPFRC) was selected for the topping slab. The UHPFRC used in this study had a compressive strength of 180 MPa and a tensile strength of 8.8 MPa, with high ductility in both tension and compression due to the crack-bridging effect of the high strength steel fibers included in the UHPFRC. Therefore steel bars are not necessary to reinforce the UHPFRC slab for shrinkage and temperature effects, thereby reducing the slab thickness and overall self-weight of the composite HFRP-UHPFRC beam system.

Ultra High Performance Fiber Reinforced Concrete (UHPFRC)

Mixture proportions of the UHPFRC are shown in Table 3. The UHPFRC is composed of water, premixed cementitious powder, sand, water reducing agent and steel fibers. The premixed cementitious powder includes ordinary Portland cement, pozzolanic materials (usually silica fume) and ettringite according to Japanese standards for blended cement.

The steel fibers have a tensile strength of 2,000 MPa and lengths of 22 mm and 15 mm. The fibers were added at approximately 1.75% volume ratio. The UHPFRC slabs were precasted and cured at 85 Celsius degrees for 24 hours. Compression tests were performed on 100x200 mm cylinders of the UHPFRC to determine compressive strength and modulus of elasticity. Moduli of rupture tests were performed on 100x100x400 mm specimens to determine the tensile strength of the UHPFRC. Three specimens were tested for each material property and the average values are listed in Table 4.

Table 3—Mix Proportions of UHPFRC

Air content (%)	Unit quantity (kg/m ³)			W.R. Admixture	Steel fiber (kg)
	Water	Premix cement	Sand		
2.0	205	1287	898	32.2	137.4

Table 4—Test Results of UHPFRC Material

Compressive strength f'_c (MPa)	Tensile strength f_t (MPa)	Young's modulus E_c (GPa)
173	14.3	48.6

Test Variables

The test variables for the full-scale beam flexural tests are shown in Table 5. Five specimens with different dimensions for the UHPFRC slab were tested. The geometry of the test specimens and the dimensions of the beam cross-sections are shown in Figures 11 and 12. The total length of each specimen is 3500 mm with the flexural and shear spans at 1000 mm as shown in Figure 11. Timber stiffeners were installed at a spacing of 500 mm on both sides of the web to prevent web buckling. The stiffeners were bonded to the HFRP specimens using epoxy bonding. Different types of shear connectors including headed bolts with/without epoxy bonding and slab anchors were tested to investigate the composite/non-composite actions between the HFRP beam and the UHPFRC slab. The spacing of headed bolts and slab anchors was determined from the shear connection tests

to prevent premature bolt shear failure as shown in Figure 13. A torque wrench was used to apply 20 N-m torque to the bolts in all specimens.

Table 5—Flexural Beam Test Variables

Specimen name	Shear connector	Epoxy bonding	Width of UHPFRC slab (mm)	Thickness of UHPFRC slab (mm)	Embedded length of bolt (mm)										
B-135-50	M16 bolt	No	135	50	35										
SA-135-50	Slab anchor	No	135	50	35										
BE-95-50	M16 bolt	Yes	50	35	BE-135-35	M16 bolt	Yes	135	35	30	BE-135-50	M16 bolt	Yes	135 <td 50	35
BE-135-35	M16 bolt	Yes	135	35	30										
BE-135-50	M16 bolt	Yes	135 <td 50	35											

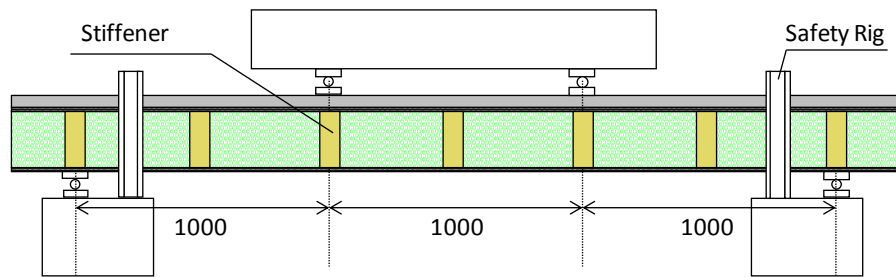
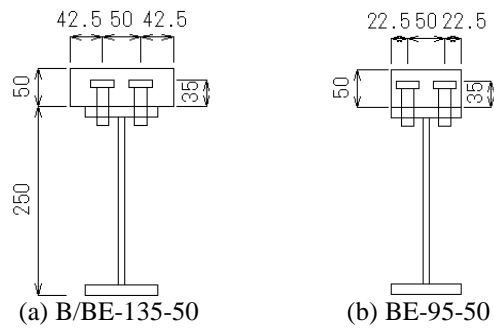


Figure 11—Geometry of specimen for flexural test



(a) B/BE-135-50

(b) BE-95-50

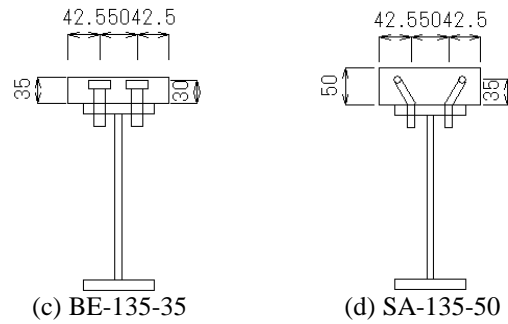


Figure 12—Dimensions of the beam cross-sections

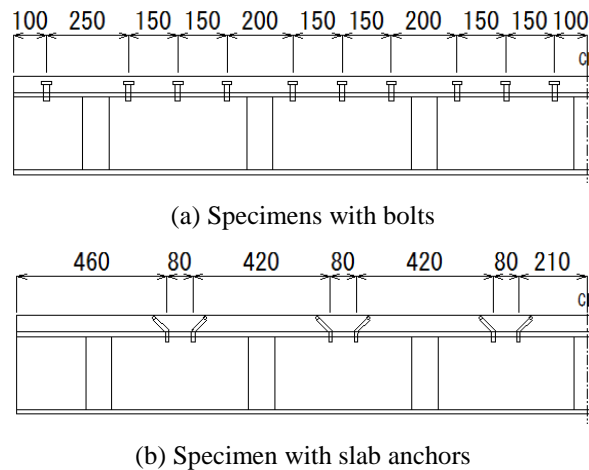


Figure 13—Locations of shear connectors

Experimental Setup and Procedure

Four point bending test was conducted on all specimens. The experimental setup is shown in Figure 14. The load was applied by a manually operated hydraulic jack until beam failure. The applied load, deflection at mid-span, and strains in the HFRP beam section were measured throughout the test.



Figure 14—Flexural beam test setup

Results and Discussion

Figure 15 shows the load and mid-span deflection relationship of each specimen. For comparison, the load-deflection relation curve for a HFRP beam without UHPFRC slab (control specimen) and a composite beam with NSC slab (specimen HFRP-NSC) are also included in Figure 15. All specimens with bolt shear connectors show higher stiffness and loading carrying capacity than the control specimen. In particular, the stiffness of specimen BE-135-50 is approximately 15% higher compared with that of specimen B-135-50. On the other hand, the specimen SA-135-50 did not perform well compared to the specimens using headed bolts. The stiffness of the load-deflection curve of specimen BE-135-50 is only 1.6 times lower than that of specimen HFRP-NSC. However, it is important to note that the total cross sectional area of the slab in specimen BE-135-50 is 5.9 times lower than that of specimen HFRP-NSC. This indicates that the use of UHPFRC slab is more effective than NSC slab in terms of structural stiffness and weight.

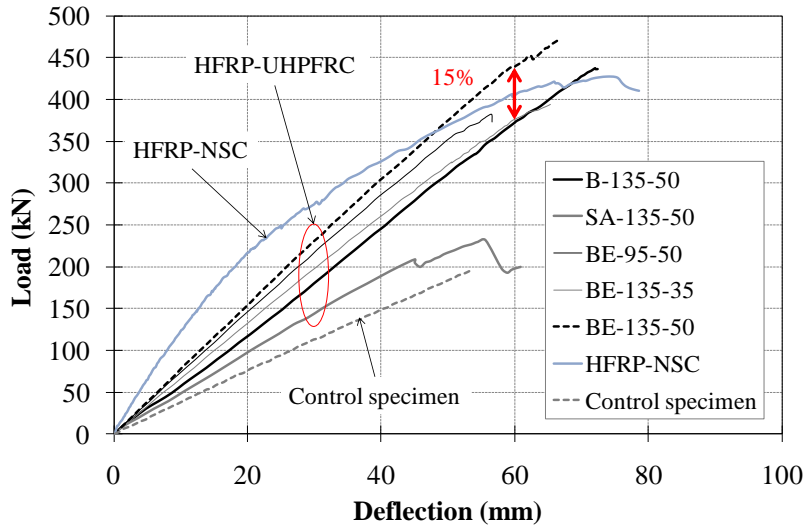


Figure 15—Load-deflection relationships

Figure 16 shows the relationship between the load and longitudinal strain through the depth of the composite beam at mid-span for various load levels, including failure load. As shown in Figure 16a, the specimen with epoxy bonding shows a linear strain distribution through the cross-section. On the other hand, Figures 16b and 16c shows slipping at the interface between the UHPFRC slab and the HFRP beam for specimen without epoxy bonding. This result indicates that specimens with bolted and bonded connection show full composite action until the final failure. The specimen with shear anchors showed even larger slip than the specimens with bolts. The results also show that at failure, the maximum tensile strain recorded at the tensile flange of the HFRP is around 10,000 microstrains. This level of strain is significantly higher than the 6,000 microstrains recorded at failure in the tensile flange of the HFRP beam tested without slab. This shows that the addition of UHPFRC slab on the HFRP beam resulted to the effective utilization of the high tensile strength of the CFRP.

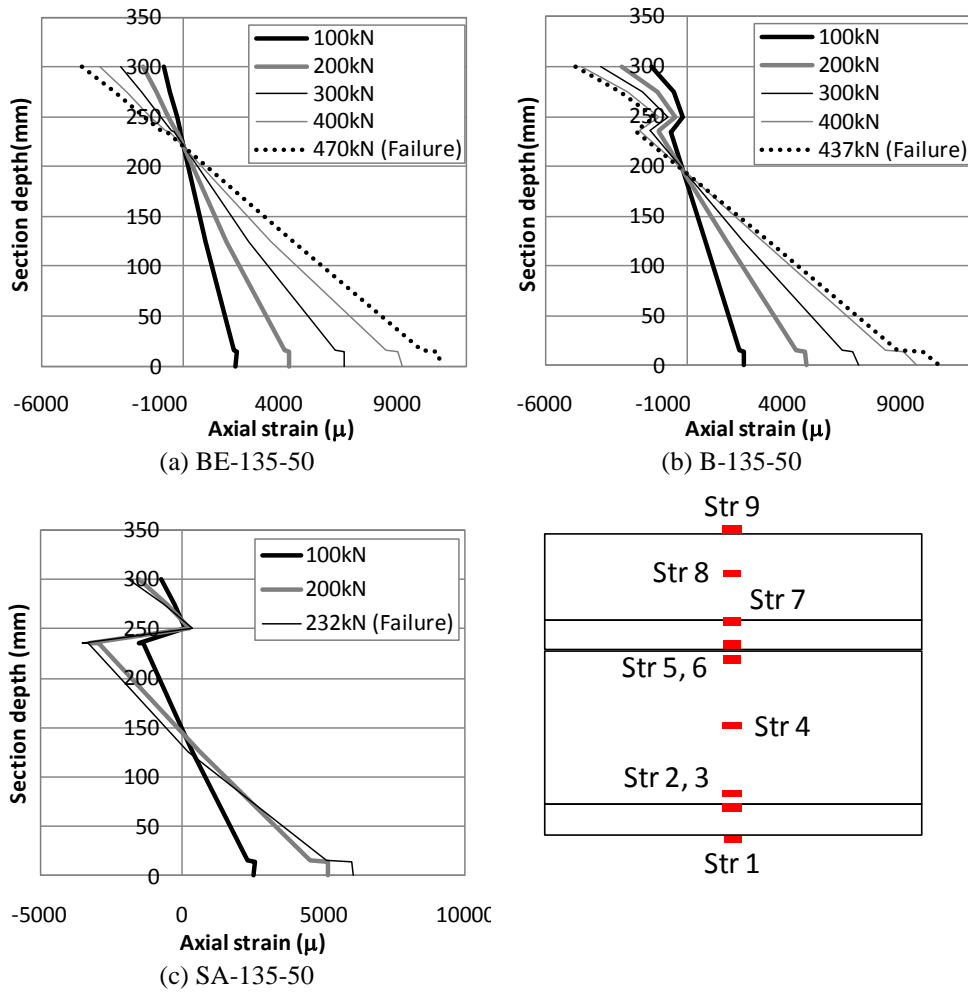
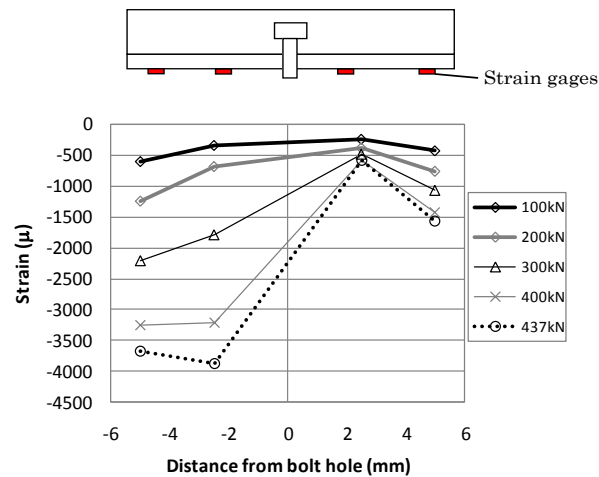


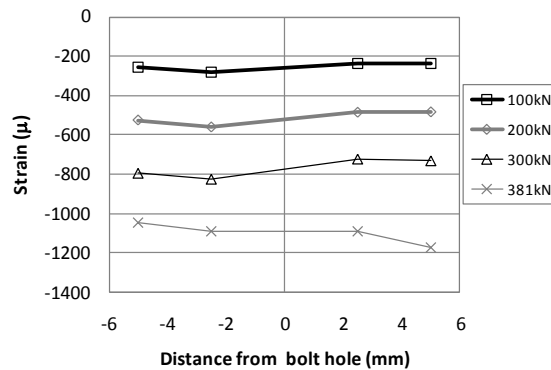
Figure 16—Longitudinal strain distribution along the depth of the composite beam

The strain distributions along the top flange of the HFRP beam near a bolt hole in the left shear span are shown in Figure 17. As shown in Figure 17a for a specimen without epoxy, the strain to the right of the bolt is small while strain to the left of the bolt shows high compression in the HFRP beam flange. This strain distribution indicates that slipping occurred at the interface between the UHPFRC slab and the HFRP beam allowing the bolts to bear against the edge of the hole to resist the horizontal shear flow. On the other hand, this behavior was not observed in specimens with epoxy bonding.

Figure 17b shows that the strains in the HFRP beam flange are uniformly distributed regardless of the bolt types and bolt hole location. These results confirm that the slipping between the UHPFRC slab and the HFRP beam was resisted by the epoxy bonding especially in the shear span where horizontal shear stress is significant. The bolts also serve to prevent peeling at the UHPFRC slab to HFRP beam interface, and to provide reserve strength if debonding occurs.



(a) Specimen without epoxy



(b) Specimen with epoxy

Figure 17—Strain distribution in HFRP top flange near bolt hole

All specimens with headed bolts failed due to crushing of the UHPFRC slab at a loading point followed by crushing of the HFRP beam flange as shown in Figure 18a.

Delamination of the top flange of the HFRP beam was observed in specimen SA-135-50 with shear anchors (Figure 18b). This failure mode is similar to that of HFRP beam without slab, however the failure was not brittle as the UHPFRC slab carried compressive force even after delamination failure occurred. In addition, a few of the slab anchors failed in shear, while the others caused bearing failure in the HFRP beam flange.

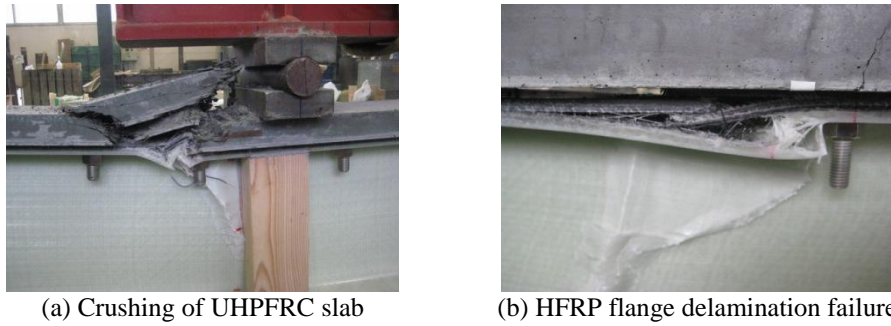


Figure 18—Failure modes of composite beams in flexure

Fiber model analysis of the HFRP-UHPFRC composite girders was conducted and the results were compared with the experimental results. Bernoulli-Euler theory was assumed in this analysis. Bi-linear stress-strain relationship from the design code for ultra high strength fiber reinforced concrete structures (Figure 19) was used to model UHPFRC (JSCE 2004).

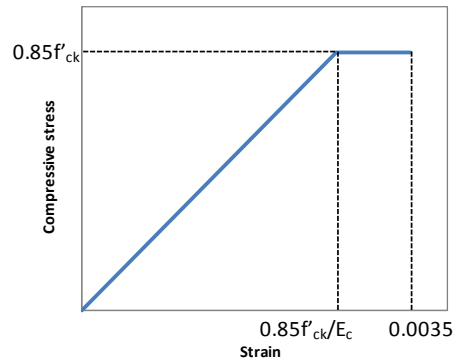


Figure 19—Bi-linear stress-strain relationship of UHPFRC

Table 6 shows comparisons between analytical and experimental results for the HFRP-UHPFRC composite beams used headed bolt and epoxy bonding as shear connectors.

The results indicated that the analytical model could well predict the failure load and failure mode of beams. The differences in failure load between the analysis and experiment are less than 5%. However, the analytical model over-estimates the stiffness of the composite beam as shown in Figure 20. According to the analytical model, compression failure of the UHPFRC slab should occur at mid-span. However, failure occurred at the loading point in the experiment and higher strains were recorded at the loading point due to stress concentration. The disagreement in stiffness between the analytical and experimental results is attributed in part to early plastic behavior at the loading point caused by this stress concentration. The analytical model assume perfect bond between the UHPFRC and HFRP, whereas the test specimens may experience some deformation at the bond interface.

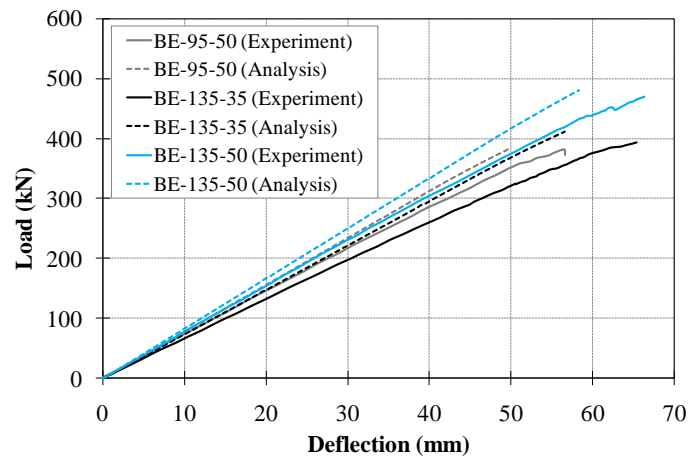


Figure 20—Comparisons of load-deflection curves between experiments and analysis

Table 6—Flexural Beam Test Results at Failure

Beam	Predicted failure load	Actual failure load	Predicted/actual failure mode
B-135-50	—	438	Compression – UHPFRC
SA-135-50	—	232	Delamination – HFRP top flange
BE-95-50	384	382	Compression – UHPFRC
BE-135-35	411	394	Compression – UHPFRC
BE-135-50	481	470	Compression – UHPFRC
HFRP-NSC	—	427	Compression – NSC

CONCLUSION

This paper presents an experimental study of HFRP beams and composite beams consisting of HFRP beams and concrete topping slabs connected by bolts or slab anchors. The main conclusions from the study are summarized as follows:

1. The investigated HFRP beams behave linearly under flexural load and failed suddenly without forewarning. The failure was crushing of fibers near the loading point due to load concentration followed by the delamination of the compressive flange between the interface of CFRP and GFRP layers.
2. Composite beams consisting of HFRP beams and concrete topping slabs significantly improve their flexural stiffness and effectively utilize the superior properties of the HFRP materials.
3. The use of UHPFRC slab is more effective than NSC slab in terms of structural stiffness and weight.
4. HFRP-UHPFRC composite beams with headed bolt shear connectors provide considerable stiffness and strength increase compared with HFRP beams without concrete topping slab.
5. Composite beams with epoxy bonding between the UHPFRC slab and HFRP beam top flange showed an approximately 15% increase in flexural stiffness than beams connected with bolts only.

ACKNOWLEDGMENTS

The authors would like to thank Kajima Corporation for providing Ultra High Performance Fiber Reinforced Concrete “SUQCEM” (Super high-Quality Cementitious Material).

REFERENCES

- Concrete Committee of Japan Society of Civil Engineers (JSCE-2004).
“Recommendations for Design and Construction of Ultra High Performance Fiber Reinforced Concrete Structures”.

- Elmahdy, A., El-Hacha, R., and Shrive, N. (2008). "Flexural behavior of hybrid composite girders for bridge construction". Proceedings of the ACI special publication on FRP stay-in-place forms for concrete structures, the ACI spring convention in Los Angeles, CA, USA.
- Hirokazu Tanaka, Hitoshi Tazawa, Morio Kurita, Takumi Shimomura (2006). "A case study on life-cycle assessment of environmental aspect of FRP structures". Proceedings of Third International Conference on FRP Composites in Civil Engineering (CICE 2006), Florida, USA, pp. 175-178.
- J.R. Correia, F.A. Branco, J.G. Ferreira (2007). "Flexural behaviour of GFRP-concrete hybrid beams with interconnection slip". *Composite Struct* 77 (1), pp. 66–78.
- Keller, T., Schaumann, E., Vallée, T. (2007). "Flexural behavior of a hybrid FRP and lightweight concrete sandwich bridge deck". *Composites Part A* 38 (3), pp. 879–889.
- Koji Sakai (2005). "Environmental Design for Concrete Structures". *Journal of Advanced Concrete Technology*, Vol.3, No.1, pp.17-28.
- Allan Manalo, Hiroshi Mutsuyoshi, Thiru Aravinthan, Takahiro Matsui (2009). "Behaviour of Hybrid FRP Composite I-Girder with Concrete Deck". FRPRCS-9, Sydney, Australia.
- Nguyen Duc Hai, Hiroshi Mutsuyoshi, Shingo Asamoto, and Takahiro Matsui (2010). "Structural Behavior of Hybrid FRP Composite I-Beam". *Journal of Construction and Building Materials*, Vol. 24, pp. 956-969.
- Nikola Deskovic, Thanasis C. Triantafillou, Urs Meier (1995). "Innovative Design of FRP Combined with Concrete: Short-Term Behavior". *J. Struct. Engrg.* Volume 121, Issue 7, pp. 1069-1078.
- Nikola Deskovic, Thanasis C. Triantafillou, Urs Meier (1995). "Innovative Design of FRP Combined with Concrete: Long-Term Behavior". *J. Struct. Engrg.* Volume 121, Issue 7, pp. 1079-1089.